PCCP

Accepted Manuscript

ROYAL SOCIETY OF CHEMISTRY

www.rsc.org/pccp

Molecular weight growth in Titan's atmosphere: branching pathways for the reaction of 1-propynyl radical ($H_3CC{\equiv}C^{\bullet}$) with small alkenes and alkynes.

Benjamin B. Kirk,[1] John D. Savee,[2] Adam J. Trevitt,[3] David L. Osborn,[2] and Kevin R. Wilson[1*]

1. Chemical Sciences Division, Lawrence Berkeley National Laboratory, 1 Cyclotron Road MS 6R2100, Berkeley CA 94720-8226

2. Combustion Research Facility, Sandia National Laboratories, Livermore CA

3. School of Chemistry, University of Wollongong, NSW Australia 2522

* Corresponding Author krwilson@lbl.gov

Abstract

The reaction of small hydrocarbon radicals (i.e. $^{\bullet}CN$, $^{\bullet}C_2H$) with trace alkenes and alkynes is believed to play an important role in molecular weight growth and ultimately the formation of Titan's characteristic haze. Current photochemical models of Titan's atmosphere largely assume hydrogen atom abstraction or unimolecular hydrogen elimination reactions dominate the mechanism, in contrast to recent experiments that reveal significant alkyl radical loss pathways during reaction of ethynyl radical ($^{\bullet}C_2H$) with alkenes and alkynes. In this study, the trend is explored for the case of a larger ethynyl radical analogue, the 1-propynyl radical ($H_3CC{\equiv}C^{\bullet}$), a likely product from the high-energy photolysis of propyne in Titan's atmosphere. Using synchrotron vacuum ultraviolet photoionization mass spectrometry, product branching ratios are measured for the reactions of 1-propynyl radical with a suite of small alkenes (ethylene and propene) and alkynes (acetylene and d_4-propyne) at 4 Torr and 300 K. Reactions of 1-propynyl radical with acetylene and ethylene form single products, identified as penta-1,3-diyne and pent-1-en-3-yne, respectively. These products form by hydrogen atom loss from the radical-adduct intermediates. The reactions of 1-propynyl radical with d_4-propyne and propene form products from both hydrogen atom and methyl loss, (-H = 27%, $-CH_3$ = 73%) and (-H = 14%, $-CH_3$ = 86%), respectively. Together, these results indicate that reactions of ethynyl radical analogues with alkenes and alkynes form significant quantities of products by alkyl loss channels, suggesting that current photochemical models of Titan over predict both hydrogen atom production as well as the efficiency of molecular weight growth in these reactions.

Introduction

The atmosphere of Saturn's moon Titan is composed primarily of nitrogen (N_2) (95 - 98%; surface to stratosphere) and methane (CH_4) (4.9 - 1.4%; surface to stratosphere) with trace quantities of hydrogen and hydrocarbons.[1] The surface pressure is higher than Earth at 1.43 atm, but due to lower gravity, the atmosphere extends more than 1000 km from the surface. In the stratosphere, complex mixtures of polycyclic aromatic hydrocarbons, clusters and aerosols have been detected, giving Titan its characteristic haze.[1]

There is much interest in the hydrocarbon growth mechanisms of Titan's haze layer, particularly how simple alkane precursors form ring-containing molecules that ultimately seed larger particles. Generalized mechanisms for molecular growth consider two general pathways. The first arises from ion chemistry – where ions are generated in the upper atmosphere by the incidence of Saturn's ionosphere and ionizing solar radiation.[2] The second general pathway results from radical chemistry from reactive carbon-centered radicals such as ethynyl ($^{\bullet}C_2H$) and cyano ($^{\bullet}CN$) radicals produced by incident non-ionizing solar radiation.[2] While both processes are believed to contribute to aerosols and aggregates in the haze layer, here we focus on the radical growth mechanism.

The highly reactive ethynyl and cyano radicals react at close to the collision limit ($\sim 10^{-10}$ cm^3 molecules^{-1} s^{-1}), even at extremely low temperatures.[3-5] Reaction of these radicals with trace alkenes and alkynes forms larger unsaturated molecules.[6,7] Elucidating the mechanism by which large highly unsaturated molecules are transformed to cyclic species such as benzene or polyaromatic hydrocarbons in cold planetary atmospheres is an ongoing challenge. However, after its detection in both Titan's upper and lower atmospheres, benzene is seen as the most likely building block from which larger polyaromatic species emanate.[2,8-10]

Haze condensates have been detected well above the main haze layers, suggesting reactions initiated by higher energy photons contribute to the

chemistry of haze formation.[2,11-13] On Titan, ethynyl radicals are considered important for molecular growth mechanisms due to the abundance of acetylene, from which it is generated.[14,15] The concentration of larger hydrocarbons in Titan's atmosphere decreases significantly with increasing carbon number; however, the concentration of larger unsaturated hydrocarbons is not insignificant. Propyne ($H_3CC{\equiv}CH$), for example, is measured in parts-per-billion concentrations in Titan's stratosphere.[14]

Photolysis of propyne ($H_3CC{\equiv}CH$) may yield the ethynyl radical analogue 1-propynyl radical ($H_3CC{\equiv}C^{\bullet}$) or propargyl radical ($^{\bullet}CH_2C{\equiv}CH$) after C-H bond homolysis of the acetylenic or methyl carbons, respectively.[16,17] Unlike the resonantly stabilized propargyl radical, 1-propynyl radical is very reactive with rate coefficients that are expected to be similar to that of the ethynyl radical. Qadari et al. reported that at 193.3 nm, photolysis of propyne generates mostly propargyl radical,[17] while a mixture of 1-propynyl and propargyl radicals were measured at Lyman-alpha wavelengths (121.6 nm).[17] However, Harich et al. found that C-H bond homolysis after 157 nm photolysis predominantly occurred from the terminal acetylenic carbon.[16] This result suggests that 1-propynyl radicals can be generated by photolysis of propyne down to ~400 km above Titan's surface (i.e. within the detached haze layer).[1,18] While the 1-propynyl radical is not expected to be formed in high concentrations, it is conceivable that when formed it would react quickly, primarily by addition to double or triple bonds to form larger molecules.

In this work, laser photolysis synchrotron photoionization mass spectrometry is used to investigate the reaction of the 1-propynyl radical with a series of C_2-C_3 alkenes (ethylene and propene) and alkynes (acetylene and d_4-propyne) at 4 Torr and 300 K. We investigate product branching ratios, in order to quantify products formed via hydrogen atom loss and alkyl radical loss channels. Quantum chemical calculations are used to support our experiments. Finally, we discuss these results in the context of current photochemical models of Titan's atmosphere.

Experimental

1-Iodopropyne (>97%) was purchased from TCI Chemicals (Portland, OR). Acetylene was purchased from Praxair (Danbury, CT). Ethylene (99.99%), and propene (≥99%) were purchased from Sigma-Aldrich (St. Louis, MO). d_4-Propyne (98%) was purchased from Cambridge Isotope Laboratories, Inc. (Tewksbury, MA).

Experiments are conducted in a slow flow reactor coupled to a synchrotron vacuum ultraviolet (VUV) time-resolved photoionization time of flight mass spectrometer. A detailed description of the instrument can be found elsewhere.[19] Briefly, small quantities of the precursor halide (1-iodopropyne) and the excess reactant are seeded into a large flow of helium at a total pressure of 4 Torr at room temperature (300 K, number density = 1.3 x 10^{17} cm^{-3}). In these experiments, helium is passed over glass wool impregnated with 1-iodopropyne (vapor pressure = 101 Torr) at a pressure of 590 Torr (20 °C) (number density = 3.3 x 10^{16} cm^{-3}). A 1 sccm flow of the diluted 1-iodopropyne (number density = 2.2 x 10^{14} cm^{-3}) is combined with 1-2 sccm of the reactant (5% acetylene, 5% ethylene, 2.4% d_4-propyne, 5% propene in helium; typical number densities = (0.3-1.3) x 10^{14} cm^{-3}) with a balance of helium generating a total flow rate of 100 sccm. 1-Propynyl radicals are generated by 248 nm pulsed photolysis of 1-iodopropyne using an unfocussed excimer laser operating at 4 or 10 Hz repetition rate. The laser fluence is between 50 - 75 mJ cm^{-2}. The reacting mixture from the flow tube is expanded through a ~650 μm diameter pinhole and sampled by a 1.5 mm diameter skimmer into the detection region of the instrument. Quasi-continuous VUV radiation from the Chemical Dynamics Beamline (Advanced Light Source, Berkeley, CA) is used for product ionization. The VUV light is dispersed by a 3 m off-plane monochromator and enters the chamber through a 100-700 μm exit slit. A slit width of 400 μm yields a photon energy resolution ~25 meV. The monochromatized radiation crosses the gas flow to ionize the reaction mixture at discrete energies. The resulting ion beam is sampled at 50 kHz by an orthogonal acceleration time of flight mass spectrometer.

450 time-resolved mass spectra are averaged at each photoionization energy. The background-subtracted spectrum is obtained by subtracting the averaged mass spectrum recorded prior to the laser pulse from the post-laser time-resolved mass spectra. Each mass spectrum presented here consists of the background-subtracted spectrum time-integrated over 60 ms after the laser pulse. Photoionization spectra were normalized to the photon flux measured at each photon energy by a NIST-calibrated photodiode (Opto Diode Corp., SXUV100).

Notably, although we measure time-resolved data, we maximize selectivity of the reactions in this study by choosing relatively large concentrations of the excess reactant, which increases the likelihood that the 1-propynyl radical ($H_3CC{\equiv}C^{\bullet}$) reacts with the excess reactant and not with the 1-iodopropyne precursor. However, this choice makes the kinetics too fast to reliably measure rate coefficients. Given this limitation, we can place a lower limit on the second order rate constant for the reactions measured here of 10^{-11} cm^3 $molecules^{-1}$ s^{-1}.

Side reactions arising from reaction of 1-propynyl radical with 1-iodopropyne were measured and are discussed in the results section. Secondary reaction products should they be formed would arise at multiples of the mass of the reactant or radical, i.e. $xR^{\bullet} + y(R' - H)$. No ions were measured with this characteristic m/z above that of the primary reaction product, thus under these conditions we do not expect secondary reactions to contribute to the product population.

A complete description of the methods employed for electronic structure calculations, complete potential energy schemes, geometries, energies and frequencies are provided as supporting information.

Results

In this section, the 248 nm photolysis of 1-iodopropyne is first described in order to confirm that the 1-propynyl radical is indeed produced under the

experimental conditions. This is followed by an investigation of 1-propynyl radical reactions with acetylene and d_4-propyne, then ethylene and propene. The products of these reactions are analyzed by comparing photoionization spectra to both experimentally and theoretically calculated ionization energies, and also by comparing experimental results to quantum chemical calculations of reaction pathways.

1. *Generation of the 1-propynyl radical and its self-reaction products*

The 1-propynyl radical ($H_3CC{\equiv}C^{\bullet}$) is 10 kcal/mol[20,21] less stable than its resonance-stabilized isomer, the propargyl radical ($^{\bullet}CH_2C{\equiv}CH$). Although it is plausible to expect that 248 nm photolysis of our precursor, 1-iodopropyne, generates 1-propynyl radical exclusively, there are no previous reports of its photochemistry. Therefore, the products arising after 248 nm photolysis of 1-iodopropyne are first investigated.

Figure 1 shows a background subtracted 10.80 eV photoionization product mass spectrum. The ions observed in this mass spectrum are assigned to propyne (m/z 40), hexa-2,4-diyne (m/z 78), atomic iodine (m/z 127), hydrogen iodide (m/z 128), iodomethane (m/z 142), 1-iodopropyne (m/z 166) and molecular iodine (m/z 254). The major time resolved signals are hexa-2,4-diyne (m/z 78) and molecular iodine (m/z 254). The assignment of these ions will be discussed further below.

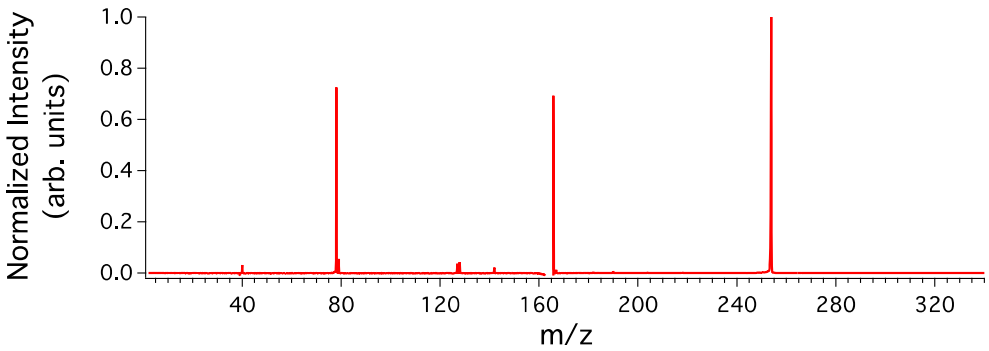

Figure 1 - Mass spectrum showing laser-induced signals obtained at 10.80 eV photoionization energy after 248 nm laser photolysis of 1-iodopropyne. The anomalous signal around m/z 166 is

due to incomplete subtraction of 1-iodopropyne, which saturates the detector at 10.80 eV. This spectrum was measured with the time-of-flight sampling rate decreased to 40 kHz to increase the mass range.

Analyzing the depletion of the iodopropyne (m/z 166) signal after the laser pulse (shown in Supporting Information, Figure S5), we estimate a photolysis yield for the iodide to 1-propynyl radical of 7 ± 1 %, for a total radical density of (1.5 ± 0.3) x 10^{13} cm^{-3}. The propargyl radical ($^{\bullet}CH_2C{\equiv}CH$) and 1-propynyl radical ($H_3CC{\equiv}C^{\bullet}$) would be detected at m/z 39; however after background subtraction there is only a small signal at this mass, with or without the addition of other reagents. Nevertheless, m/z 78 is observed, consistent with radical recombination ($C_3H_3^{\bullet} + C_3H_3^{\bullet} \rightarrow C_6H_6$) or a radical + precursor reaction ($C_3H_3^{\bullet} + H_3CC{\equiv}CI \rightarrow C_6H_6 + I^{\bullet}$).

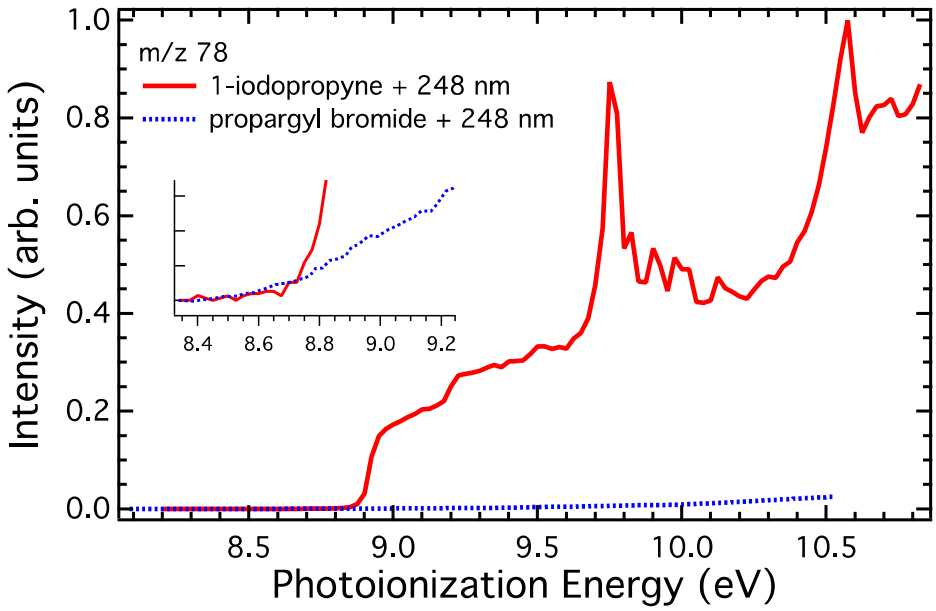

Figure 2 - Photoionization spectrum measured at m/z 78 after 248 nm laser photolysis of 1-iodopropyne and propargyl bromide.[22] Inset shows fit of the m/z 78 photoionization spectrum measured after 248 nm photolysis of propargyl bromide to arising from 1-iodopropyne.

Shown in Figure 2 are photoionization spectra of m/z 78 measured after 248 nm laser photolysis of 1-iodopropyne and propargyl bromide (a clean photolysis

precursor of propargyl radicals).[22] The inset in Figure 2 illustrates that after 8.70 eV the two traces diverge. Comparing these spectra demonstrates that the product(s) arising after photolysis of 1-iodopropyne are very different from those following propargyl bromide photolysis. This observation implies that there is little propargyl radical ($^{\bullet}CH_2C{\equiv}CH$) present in these experiments.

Calculated and experimental photoionization energies for relevant C_6H_6 (m/z 78) isomers are presented in Table S1 (Supporting Information). While the major photoionization onset observed in Figure 2 occurs at 8.85 eV, consistent with the adiabatic ionization energy (AIE = 8.90 ± 0.02 eV)[23] of hexa-2,4-diyne, a weaker earlier onset at 8.40 eV may represent fulvene (AIE = 8.36 ± 0.02 eV)[23]; however, this signal is extremely small and not further considered. The formation of hexa-2,4-diyne is consistent with radical recombination of 1-propynyl radicals ($H_3CC{\equiv}C^{\bullet} + H_3CC{\equiv}C^{\bullet} \rightarrow H_3CC{\equiv}C\text{-}C{\equiv}CCH_3$) or the radical substitution reaction of 1-propynyl radical with 1-iodopropyne ($H_3CC{\equiv}C^{\bullet} + H_3CC{\equiv}CI \rightarrow H_3CC{\equiv}C\text{-}C{\equiv}CCH_3 + I^{\bullet}$).

The photoionization spectrum of the m/z 78 product from 1-iodopropyne photolysis shown in Figure 2 contains two characteristic sharp features at 9.750 eV and 10.575 eV that likely arise from autoionizing Rydberg states converging to excited electronic states of the cation. The presence of these spectral features further supports the assignment of this ion as hexa-2,4-diyne, since analogous diynes, diacetylene (1,3-butadiyne),[24] and penta-1,3-diyne (methyl diacetylene, vida infra), exhibit similar resonances. No such features were observed in the photoionization spectrum arising from self-reaction of the propargyl radical,[22] suggesting this product is unique to reactions of 1-propynyl radical. We therefore conclude that photolysis of 1-iodopropyne results predominantly in formation of 1-propynyl radical, which then reacts with 1-iodopropyne or another 1-propynyl radical to form hexa-2,4-diyne. In either case, it does not appear that propargyl radicals are produced in any significant amount.

2. *Reaction of 1-propynyl radical with alkynes (acetylene and d_4-propyne)*

Reactions of propargyl radicals ($^{\bullet}CH_2C{\equiv}CH$) with closed-shell molecules are exceedingly slow, while the self-reaction ($^{\bullet}CH_2C{\equiv}CH + {}^{\bullet}CH_2C{\equiv}CH \rightarrow C_6H_6$) is significantly faster, with a measured room temperature rate constant of k = 4.07 x 10^{-11} cm^3 $molecule^{-1}$ s^{-1}.[25] By contrast, previous measurements of the reaction between the propargyl radical and acetylene ($^{\bullet}CH_2C{\equiv}CH + C_2H_2$) by Knyazev and Slagle found the reaction to proceed with a second-order rate constant k ~ 6.7 x 10^{-16} cm^3 $molecules^{-1}$ s^{-1} at 800 K.[26] This reaction has a positive temperature coefficient and would thus be expected to react even more slowly at room temperature. We are therefore confident that under current experimental conditions, the products that are measured arise from reactions of 1-propynyl radical.

2.1 Reaction of 1-propynyl radical with acetylene ($H_3CC{\equiv}C^{\bullet} + C_2H_2$)

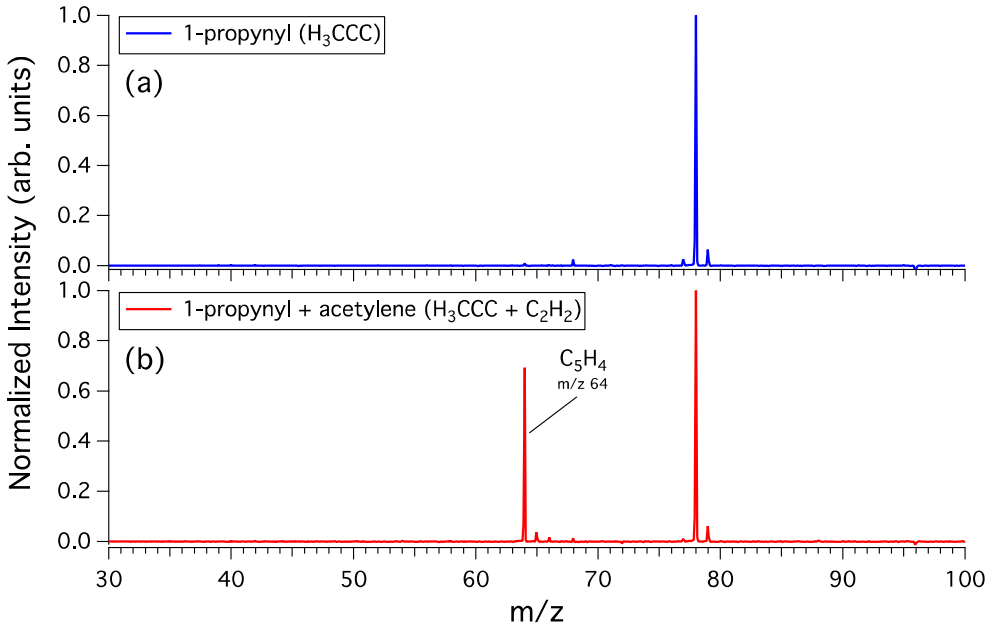

Figure 3 – 10.0 eV photoionization mass spectra measured after photolysis of 1-iodopropyne (a) without acetylene present (i.e. side and self-reaction of 1-proynyl radical) and (b) with acetylene. The major ion at m/z 64 is consistent with addition of 1-propynyl to acetylene followed by loss of $H^{\bullet}$ ($H_3CC{\equiv}C^{\bullet} + C_2H_2 \rightarrow C_5H_4 + H^{\bullet}$).

Figure 3 compares the product mass spectra observed in the presence (b) and the absence (a) of acetylene at 10.0 eV. The only observed product of the 1-propynyl + acetylene reaction appears at m/z 64 (C_5H_4) and is consistent with propynyl addition to acetylene followed by the elimination of atomic hydrogen ($H_3CC{\equiv}C^{\bullet} + C_2H_2 \rightarrow C_5H_4 + H^{\bullet}$). A photoionization spectrum for this product measured between 8.3 - 10.2 eV is shown in Figure 4 with relevant ionization energies for C_5H_4 isomers summarized in Table S2 (Supporting Information). The major onset near 9.48 eV is assigned to penta-1,3-diyne (methyl diacetylene), consistent with experimental measurement of its AIE (9.50 ± 0.02 eV)[23] and a computed AIE at the CBS-QB3 level ($AIE_{CBS\text{-}QB3}$ = 9.47 eV). There is a small onset of signal at 8.70 eV that may be due to the formation of penta-1,2,3,4-tetraene (AIE = 8.67 eV)[23]; however, this signal contributes less than 1 % of the total signal.

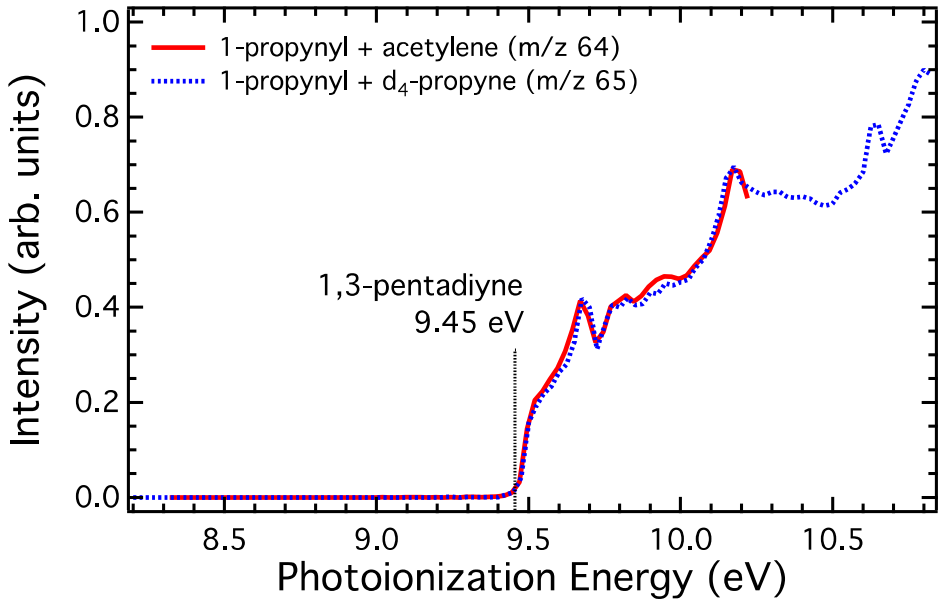

Figure 4 - Photoionization spectrum arising from reaction of 1-propynyl radical with acetylene (m/z 64) and d_4-propyne (m/z 65).

Figure 4 also shows the photoionization spectrum measured at m/z 65 from the 1-propynyl radical ($H_3C{\equiv}C^{\bullet}$) + d_4-propyne ($D_3CC{\equiv}CD$) reaction, which will be discussed in more detail below. The good agreement between the shapes of these two spectra implies that the same isomer is being produced in both

reactions. Furthermore, if the spectra in Figure 4 had significant contributions from two (or more) isomers, one would have to conclude that the branching fractions of these multiple isomers were essentially the same in these two reactions in order to produce spectra with identical shapes. A much more likely reason for this situation is that only a single, common isomer of C_5H_4 is produced in both reactions. There are characteristic features at 9.68, 10.18 and 10.65 eV in the photoionization spectra shown in Figure 4, which are likely due to autoionizing resonances. As both diacetylene[24] and hexa-2,4-diyne exhibit similar features and contain conjugated triple-bonds, it appears to be a general feature in the spectra of diynes. These resonances contribute significantly to the photoionization spectra for this functional group and provide further evidence supporting assignment of the m/z 64 photoionization spectrum to penta-1,3-diyne.

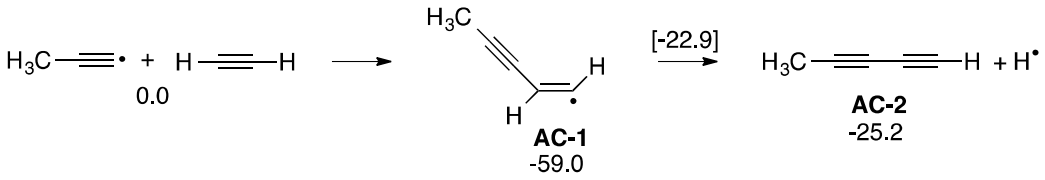

Scheme 1 - Mechanism for reaction of 1-propynyl radical with acetylene. Additional pathways are depicted in Figure S1 (Supporting Information). Energies (kcal/mol) were calculated at the CBS-QB3 level.

A potential energy scheme of the reaction, shown in the Supporting Information (Figure S1), supports these conclusions. A truncated scheme of the active pathway is shown in Scheme 1. Identifiers (**AC-x**) for the molecules are defined in Scheme 1 and Figure S1 (Supporting Information). Addition of 1-propynyl radical to the acetylene triple bond results in formation of pent-1-en-3-yn-1-yl radical (**AC-1**, Scheme 1). The lowest barrier following formation of **AC-1** is ring closure to form the three-membered ring eth-2-ylylidenecyclopropene (**AC-4**, Figure S1) with a barrier -32.0 kcal/mol below the entrance channel. No products are energetically accessible from this intermediate, so the cyclopropene intermediate will ring-open to reform **AC-1**. This could result in scrambling of the CH groups, but in this case could not be detected experimentally. The most energetically accessible pathway is thus hydrogen elimination with a barrier

residing -22.9 kcal/mol below the entrance channel to form penta-1,3-diyne (**AC-2**, Scheme 1) with a reaction exoergicity of -25.2 kcal/mol.

Although a 1,6-hydrogen atom transfer from **AC-1** is exoergic, the barrier for this process (-11.1 kcal/mol below the entrance channel) is higher than that of direct hydrogen elimination and is not likely to be competitive. Two molecules that could result from this isomerization and which have lower ionization energies, penta-1,2,3,4-tetraene (**AC-6**, Figure S1, AIE = 8.67 eV) and penta-1,2-dien-4-yne (**AC-8**, Figure S1, $AIE_{CBS\text{-}QB3}$ = 9.21 eV) are not observed in our experiments. Therefore, both experiment and theory support that the dominant product is penta-1,3-diyne (**AC-2**).

2.2 Reaction of 1-propynyl radical with d_4-propyne ($H_3CC{\equiv}C^{\bullet} + C_3D_4$)

The product formed via the hydrogen elimination channel from reaction of 1-propynyl radical ($H_3CC{\equiv}C^{\bullet}$) with propyne (C_3H_4) has the formula C_6H_6, arising in our mass spectrum after photoionization at m/z 78. Consequently, it would be obscured by the m/z 78 signal from 1-propynyl radical self- and side-reactions described above. Therefore we investigated this reaction using the perdeuterated analogue, d_4-propyne. We assume no kinetic isotope effect in the following analysis. A product mass spectrum measured at 10.80 eV is shown in Figure 5(b), which reveals two major product ions at m/z 81 and m/z 65 assigned to elimination of a deuterium atom ($H_3CC{\equiv}C^{\bullet} + C_3D_4 \rightarrow C_6H_3D_3 + D^{\bullet}$) and elimination of a d_3-methyl radical ($H_3CC{\equiv}C^{\bullet} + C_3D_4 \rightarrow C_5H_3D + CD_3^{\bullet}$) from the nascent 1-propynyl + d_4-propyne adduct.

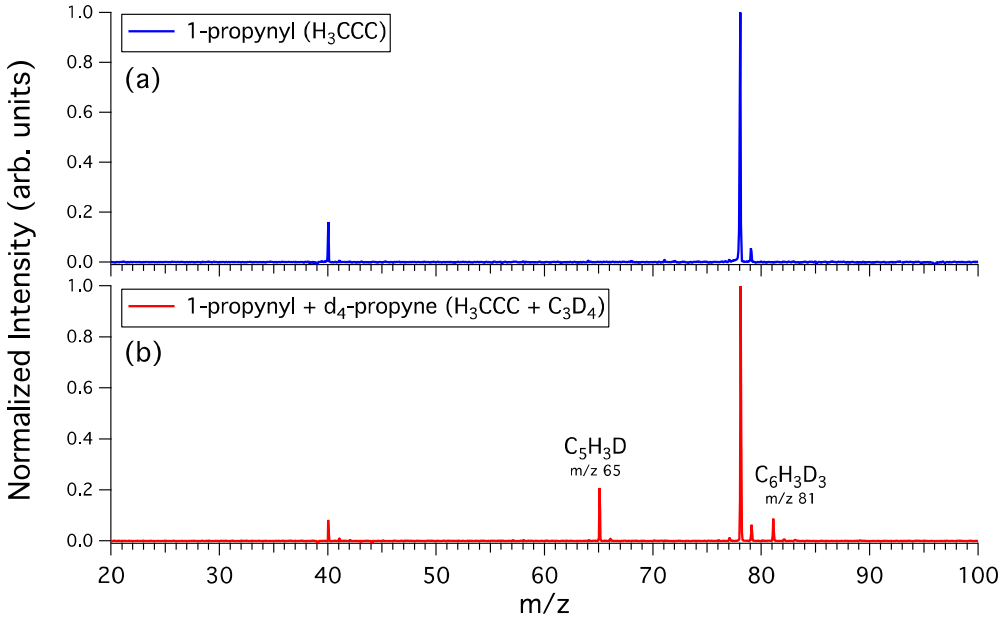

Figure 5 – 10.80 eV photoionization mass spectra measured after 248 nm photolysis of (a) 1-iodopropyne and for reaction of 1-propynyl radical with (b) d_4-propyne. The major ions at m/z 81 and m/z 65 are consistent with addition of 1-propynyl radical to d_4-propyne followed by loss of D• (i.e., $H_3CC{\equiv}C^{\bullet} + C_3D_4 \rightarrow C_6H_3D_3 + D^{\bullet}$) or $^{\bullet}CD_3$ ($H_3CC{\equiv}C^{\bullet} + C_3D_4 \rightarrow C_6H_3D + {}^{\bullet}CD_3$), respectively.

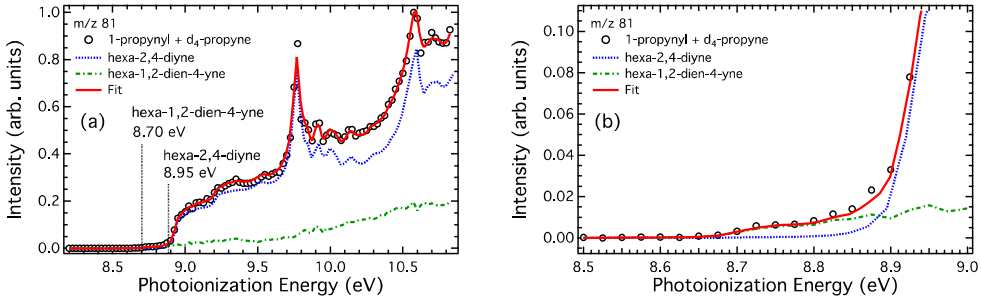

Figure 6 - Photoionization spectra measured at (a) m/z 81 with fit to hexa-2,4-diyne and hexa-1,2-dien-4-yne and (b) magnified onset region, after reaction of 1-propynyl radical with d_4-propyne.

Figure 4 shows the photoionization spectrum of the m/z 65 (C_5H_3D) ions from this reaction compared to m/z 64 (C_5H_4) spectrum from the 1-propynyl + acetylene reaction. As detailed in the previous section, we assign this species as penta-1,3-diyne, exclusively. The m/z 81 ($C_6H_3D_3$) photoionization spectrum (Shown in Figure 6a) exhibits two onsets at 8.70 eV (minor) and 8.95 eV (major) (magnified onset region shown in Figure 6b), consistent with the

photoionization energies of hexa-1,2-dien-4-yne ($AIE_{CBS\text{-}QB3}$ = 8.70 eV) and hexa-2,4-diyne (AIE = 8.90 ± 0.02),[23] respectively. The peaks at 9.74 eV and 10.56 eV are consistent with the photoionization spectrum of hexa-2,4-diyne as shown in Figure 2.

The assignment of the second isomer as hexa-1,2-dien-4-yne as a single additional product is supported by experiments of the 1-propynyl radical with 1-butyne. A detailed discussion of this reaction will be provided in a future publication, but briefly, the reaction of 1-propynyl radical with 1-butyne yields a C_6H_6 product (m/z 78) after $^{\bullet}CH_3$ loss, that we expect to be hexa-1,2-dien-4-yne (Supporting Information, Figure S6). Subtracting the reference hexa-2,4-diyne photoionization spectrum from the m/z 78 signal in either the 1-propynyl + 1-butyne reaction or the 1-propynyl radical + d_4-propyne reaction yields identical residuals (Supporting Information, Figure S7). If a significant quantity of a second isomer were present, it is highly unlikely these residuals would be the same. The photoionization spectrum for hexa-1,2-dien-4-yne shown in Figure 6 is the average of these two residual spectra (Supporting Information, Figure S7). Therefore, the fit to the photoionization spectrum measured at m/z 78 from the 1-propynyl radical + d_4-propyne reaction (Figure 6) was calculated by a least-squares routine with the estimated hexa-1,2-dien-4-yne and hexa-2,4-diyne photoionization spectra as pure isomer basis functions.

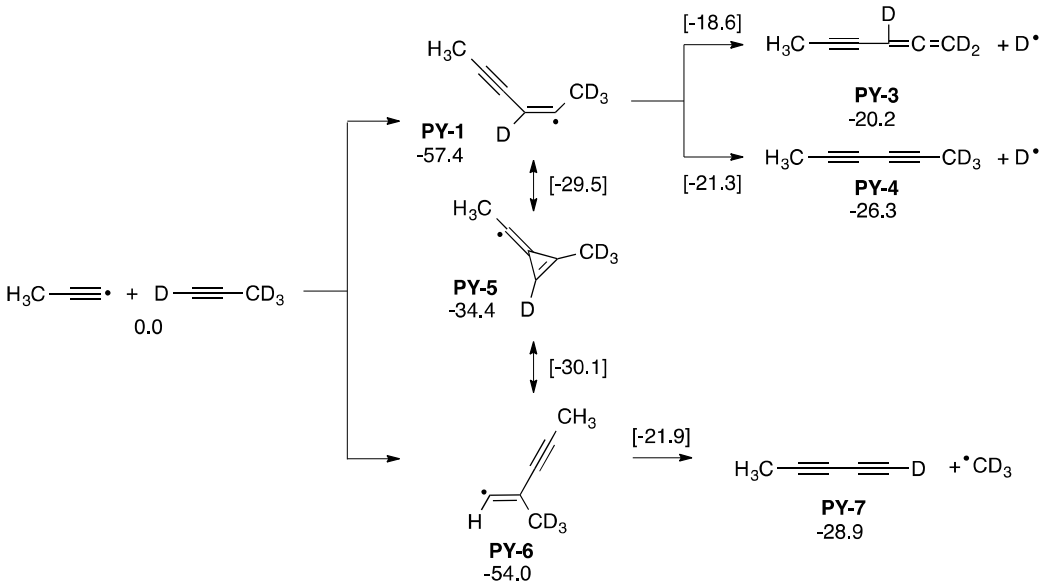

Scheme 2 - Overall reaction scheme for reaction between 1-propynyl radical with d_4-propyne. Additional pathways are depicted in Figure S2 (Supporting Information). Energies (kcal/mol) were calculated at the CBS-QB3 level.

Potential energy calculations for this reaction are presented in Figure S2 (Supporting Information), while an abbreviated scheme depicting the active channels is shown in Scheme 2. Identifiers (**PY-x**) are defined in Scheme 2 and Figure S2. Addition of 1-propynyl radical to the terminal carbon of propyne forms the hex-2-en-4-yn-2-yl radical (**PY-1**, Scheme 2). Hydrogen atom elimination may occur from three distinct carbon atoms in this adduct. Loss of hydrogen from the methyl group originally on d_4-propyne results in the formation of hexa-1,2-dien-4-yne (**PY-3**, Scheme 2) with a barrier -18.6 kcal/mol below the entrance channel. Elimination of the originally acetylenic hydrogen on d_4-propyne (-21.3 kcal/mol barrier) forms hexa-2,4-diyne (**PY-4**, Scheme 2). 1,2-Hydrogen atom transfer from **PY-1** to form hex-2-en-4-yn-1-yl radical (**PY-2**, Figure S2) requires traversal over a barrier at -14.6 kcal/mol; however, energetically accessible products, including fulvene (**PY-14**, Figure S2; $AIE_{CBS\text{-}QB3}$ = 8.42 eV) and hexa-1,2,3,5-tetraene (**PY-15**, Figure S2; $AIE_{CBS\text{-}QB3}$ = 8.35 eV), were not measured, suggesting this reaction pathway is not active.

In contrast, addition of 1-propynyl radical to the internal-carbon of the double bond results in formation of 2-methylpent-1-en-3-yn-1-yl radical (**PY-6**, Scheme

2). The only pathways to products available are loss of a methyl radical to form penta-1,3-diyne (**PY-7**, Scheme 2) with a barrier at -21.9 kcal/mol or a 1,3-hydrogen atom transfer with a higher barrier (-16.1 kcal/mol) to form the 2-methylenepent-3-yn-1-yl radical (**PY-8**, Figure S2). Isomerization between **PY-1** and **PY-6** through 2-ethylylidene-1-methylcyclopropene (**PY-5**, Scheme 2) is possible over a barrier lower than those for product formation from **PY-1** or **PY-6**. Passage through this intermediate could facilitate scrambling between the initial terminal and central addition adducts. Note that hydrogen elimination from **PY-5** is endoergic, with the formation of 2-ethenylidene-1-methylcyclopene (**PY-14**, Figure S2) residing 3.9 kcal/mol above the entrance channel. Master equation modeling would be required to quantify the total flux through these pathways and thus the temperature and pressure dependence of the branching between **PY-3**, **PY-4** and **PY-7**.

In all, the products measured experimentally can be rationalized from the reaction pathways predicted to encounter the lowest barriers, i.e. loss of H to form hexa-1,2-dien-4-yne and hexa-2,4-diyne after addition to terminal acetylenic carbon, and loss of $^{\bullet}CH_3$ yielding penta-1,3-diyne after addition to the internal acetylenic carbon. Interestingly, while hydrogen atom transfer is energetically accessible in these reactions, products arising from such reaction pathways (i.e. from **PY-2** or **PY-8**) were not observed, possibly reflecting the low entropy of these isomerization barriers compared to the higher entropy of bond fission processes.

3. *Reaction of 1-propynyl radical with alkenes (ethylene and propene)*

3.1 Reaction of 1-propynyl radical with ethylene ($H_3CC{\equiv}C^{\bullet} + C_2H_4$)

A product mass spectrum measured at 10.80 eV after allowing 1-propynyl radical to react in the presence of ethylene is shown in Figure 9(b). The m/z 66 (C_5H_6) ion is the only product observed and is consistent with addition of 1-propynyl radical to ethylene and subsequent elimination of a hydrogen atom. A photoionization spectrum measured at m/z 66 is shown in Figure 10. The onset

at 8.95 eV is consistent with the experimental adiabatic ionization energy of pent-1-en-3-yne (AIE = 9.00 ± 0.01 eV;[27] $AIE_{CBS\text{-}QB3}$ = 8.99 eV), which is assigned as the only product based on arguments below. In addition, the photoionization spectrum of this C_5H_6 product is identical in the reaction of 1-propynyl with both ethylene and propene, supporting that it arises from a single isomer of C_5H_6.

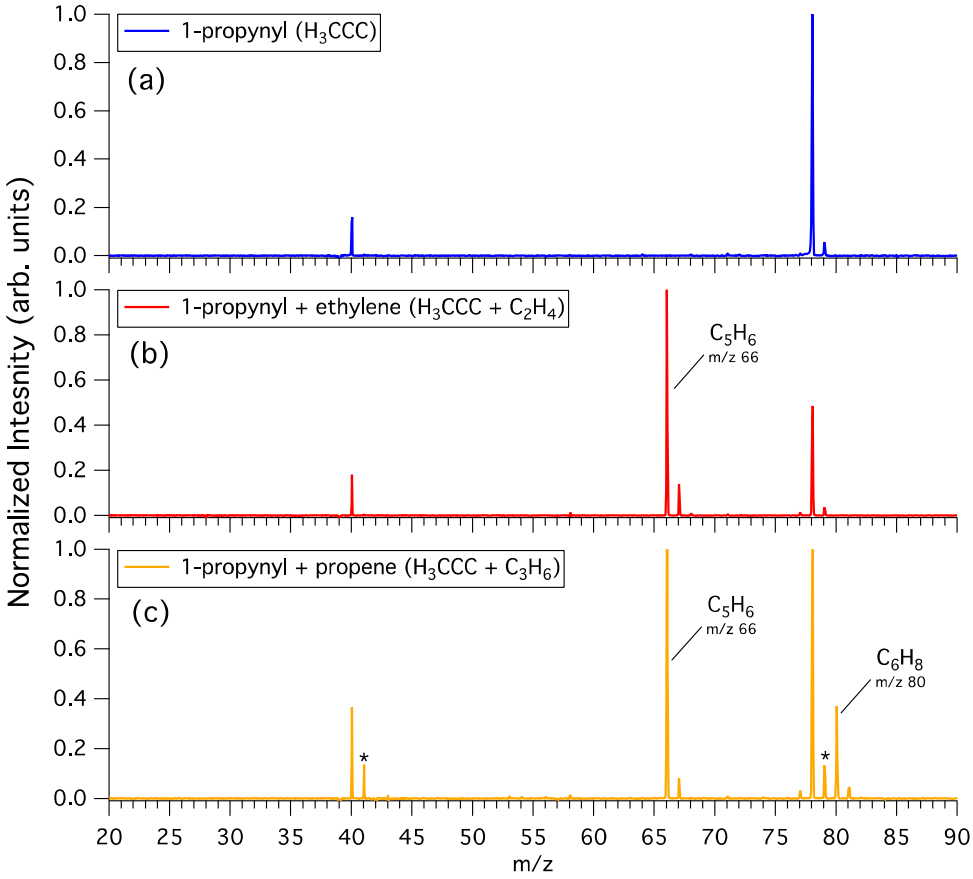

Figure 7 - Mass spectra measured at 10.8 eV after 248 nm photolysis of 1-iodopropyne (a) with no added excess reactant, (b) with added ethylene, (c) with added propene. Reaction of 1-propynyl radical with ethylene results in a single ion at m/z 66 consistent with addition of 1-propynyl radical to ethylene followed by loss of H• (i.e., $H_3CC{\equiv}C^{\bullet} + C_2H_4 \rightarrow C_5H_6 + H^{\bullet}$). Addition of 1-propynyl radical to propene results in ions at m/z 80 and m/z 66 consistent with addition and loss of H• (i.e., $H_3CC{\equiv}C^{\bullet} + C_3H_6 \rightarrow C_6H_8 + H^{\bullet}$) or •$CH_3$ (i.e., $H_3CC{\equiv}C^{\bullet} + C_3H_6 \rightarrow C_5H_6 + {}^{\bullet}CH_3$), respectively. (*) Asterisks indicate -1 Da and -39 Da dissociative photoionization products ($[M - H]^+$ at m/z 79 and $[M - C_3H_3^{\bullet}]^+$ at m/z 41, respectively) arising from the m/z 80 molecular ion.

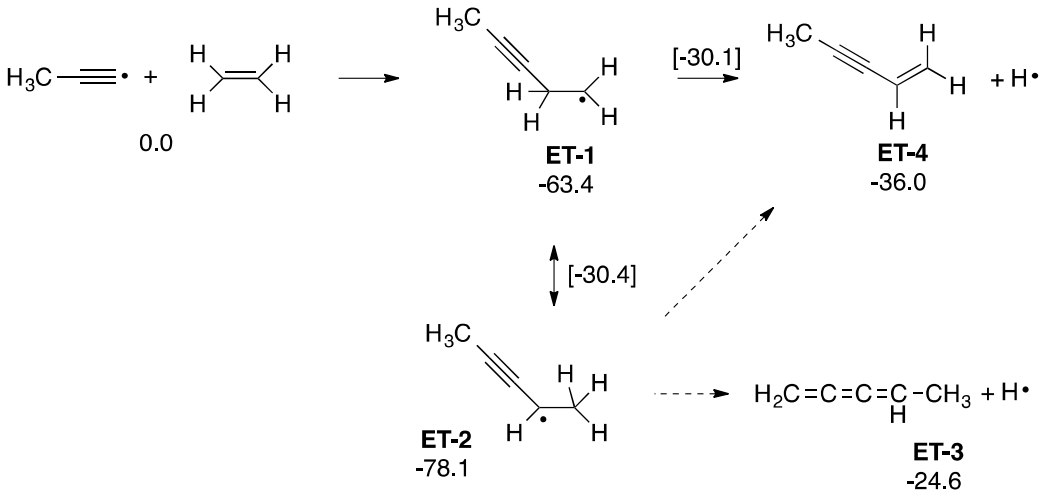

Scheme 3 - Reaction of 1-propynyl radical with ethylene. Additional pathways are depicted in Figure S3 (Supporting Information). Energies (kcal/mol) were calculated at the CBS-QB3 level.

A potential energy scheme detailing reaction pathways is provided in Figure S3 (Supporting Information). A figure detailing the active channels is presented in Scheme 3. Identifiers (**ET-x**) are defined in Scheme 3 and Figure S3. The addition of 1-propynyl radical to ethylene results in formation of pent-3-yn-1-yl radical (**ET-1**, Scheme 3) that may either eliminate hydrogen to form pent-1-en-3-yne (**ET-4**, Scheme 3), or undergo 1,2- or 1,5-hydrogen atom abstraction to form pent-2-yn-3-yl (**ET-2**, Figure S3) or pent-2-yn-1-yl radical (**ET-6**, Figure S3), respectively. The hydrogen elimination channel proceeds over a barrier at -30.1 kcal/mol with a reaction exoergicity of -36.0 kcal/mol. The 1,2-hydrogen atom transfer proceeds via a barrier at -30.4 kcal/mol, whereas 1,5-hydrogen atom transfer must overcome a barrier at -13.0 kcal/mol. The latter is energetically and entropically least favorable. The barrier for 1,2-hydrogen atom transfer encountered to generate pent-2-yn-4-yl radical (**ET-2**, Figure S3) is equal (within uncertainty) to that for direct hydrogen atom elimination to form pent-1-en-3-yne (**ET-4**, Scheme 3). Hydrogen elimination from **ET-2** can generate either penta-1,2,3-triene (**ET-3**, Figure S3) or pent-1-en-3-yne (**ET-4**). No saddle points were located for the **ET-2** to **ET-3** and **ET-2** to **ET-4** pathways at the B3LYP/CBSB7 level. The reaction energy of the hydrogen elimination pathway from **ET-2** to **ET-3** (-24.6 kcal/mol) is higher than the reaction energy of **ET-2** to **ET-4** + H (-36.0 kcal/mol). In addition, the product asymptote of the former reaction pathway is higher in energy than the barrier separating **ET-4** from **ET-1**

(-30.1 kcal/mol). Taken together, we expect the products resulting from **ET-1** and **ET-2** to be the same, i.e. pent-1-en-3-yne (**ET-4**). These calculations therefore predict that pent-1-en-3-yne (**ET-4**) should be the major product, consistent with our experimental observations.

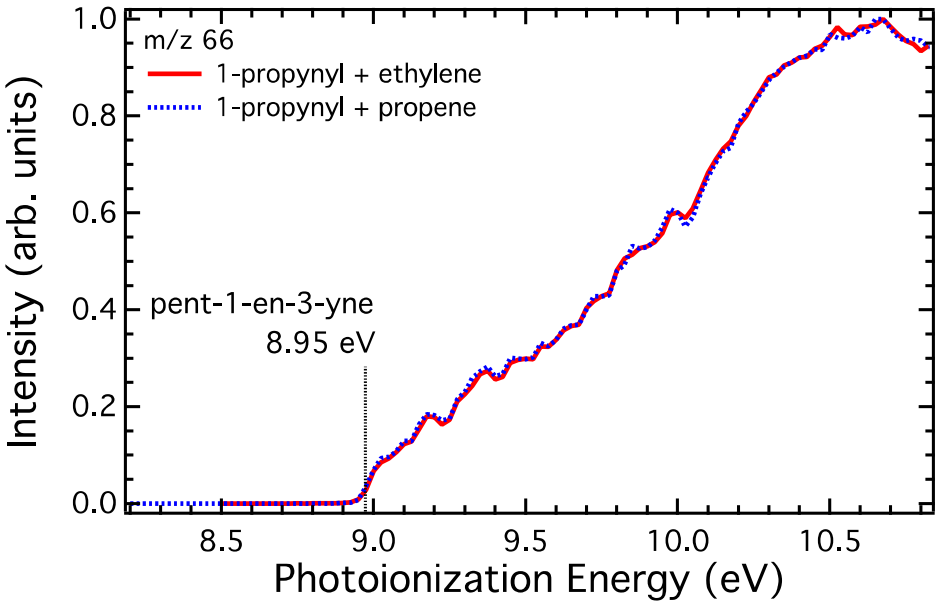

Figure 8 - Photoionization spectrum arising at m/z 66 (C_5H_6) after reaction of 1-propynyl with ethylene and propene.

3.2 Reaction of 1-propynyl radical with propene ($H_3CC{\equiv}C^{\bullet} + C_3H_6$)

When 1-propynyl radical is generated in the presence of propene, ions at m/z 80 (C_6H_8) and m/z 66 (C_5H_6) are observed, as shown in Figure 9c. These mass channels are consistent with addition of 1-propynyl radical to propene and elimination of a hydrogen atom ($H_3CC{\equiv}C^{\bullet} + C_3H_6 \rightarrow C_6H_8 + H^{\bullet}$) or a methyl radical ($H_3CC{\equiv}C^{\bullet} + C_3H_6 \rightarrow C_5H_6 + CH_3^{\bullet}$). As shown in Figure 10, the photoionization spectrum at m/z 66 is identical to that measured during reaction of 1-propynyl radical with ethylene and is therefore assigned as pent-1-en-3-yne. Ions measured at m/z 79 and m/z 41 are assigned as dissociative photoionization products. The ion at m/z 79 cannot arise from m/z 66, while photoionization of pent-1-en-3-yne (C_5H_6) yields a single ion at m/z 66 (vide supra), thus both ions must arise from dissociative photoionization of the C_6H_8 product at m/z 80. The

photoionization spectrum measured at m/z 80 is shown in Figure 11. An onset at 8.55 eV is consistent with formation of hex-2-en-4-yne, which has as calculated ionization energy of $AIE_{CBS\text{-}QB3}$ = 8.55 eV.

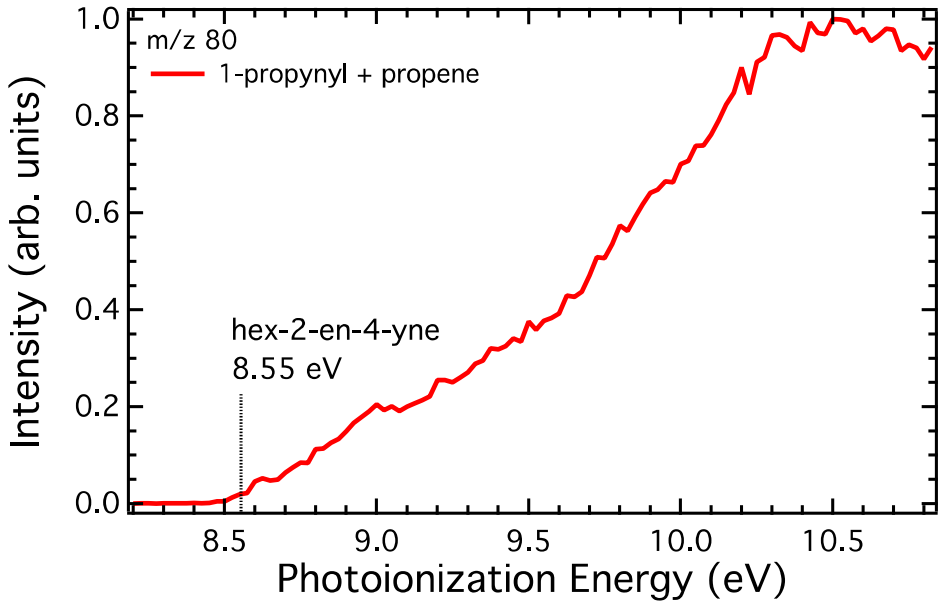

Figure 9 - Photoionization spectra measured at m/z 80 (C_6H_8) after reaction of 1-propynyl radical with propene and 1-butene.

Stationary points calculated for reaction pathways resulting in the proposed products are shown in Figure S4 (Supporting Information). A truncated scheme is presented in Scheme 4. Identifiers (**PE-x**) are defined in Figure S4 and Scheme 4. Addition of 1-propynyl radical to the terminal carbon of propene results in formation of hex-4-yn-2-yl radical (**PE-1**, Scheme 4). Hydrogen elimination may proceed from the carbon atoms adjacent to the radical site: loss from the CH_2 group originally on propene proceeds via a barrier residing -30.9 kcal/mol below the entrance channel to form the conjugated molecule hex-2-en-4-yne (**PE-3**, Scheme 4) with a reaction exoergicity of -34.0 kcal/mol. Loss of a hydrogen atom from the CH_3 group originally on propene leads to the less stable product hex-1-en-4-yne (**PE-2**, Figure 4) with reaction exoergicity of -28.5 kcal/mol.

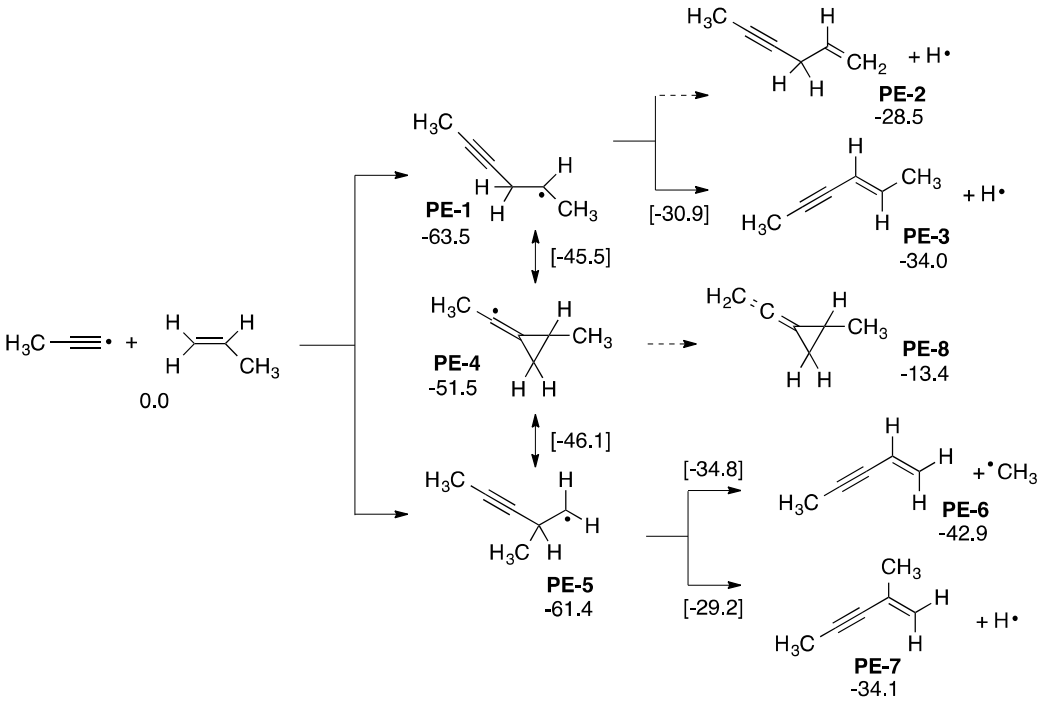

Scheme 4 - Reaction scheme for 1-propynyl radical + propene. Additional pathways are depicted in Figure S4 (Supporting Information). Dashed lines indicate channels where no barrier was located at the B3LYP/CBSB7 level. Energies (kcal/mol) were calculated at the CBS-QB3 level.

Addition of 1-propynyl radical to the internal carbon of propene results in formation of 2-methylpent-3-yn-1-yl radical (**PE-5**, Scheme 4), where hydrogen or methyl elimination are considered as the likely reaction pathways. Hydrogen elimination from the β-carbon proceeds via a barrier at -29.2 kcal/mol to form 2-methylpent-1-en-3-yne (**PE-7**, Scheme 4) with reaction exoergicity of -34.1 kcal/mol, while methyl loss requires passage over a barrier at -34.8 kcal/mol to form pent-1-en-3-yne (**PE-6**, Scheme 4) with an exoergicity of -42.9 kcal/mol.

Isomerization between **PE-1** and **PE-5** requires passage over forward barriers at -45.5 and -46.1 kcal/mol, respectively. The intermediate radical, 1-ethylyl-2-methylcyclopropane (**PE-4**) may eliminate hydrogen to form 1-ethenylidene-2-methylcyclopropane (**PE-8**) with a reaction exoergicity of -13.4 kcal/mol. Despite the **PE-8** product asymptote residing below the energy of the reactants, it is significantly higher than the two ring-opening barriers of **PE-4**, thus this pathway is not favorable. These calculations therefore predict the major product formed at m/z 80 to be hex-2-en-4-yne (**PE-3**), while pent-1-en-3-yne (**PE-6**) is

predicted to form at m/z 66. While 2-methylpent-1-en-4-yne (**PE-7**) is energetically accessible, in addition to having a higher barrier than the pathway to **PE-6**, the methyl loss transition state is expected to be entropically favored over hydrogen elimination, thus a significant contribution from this isomer at m/z 80 is not expected.

Discussion

Estimated branching ratios are shown in Table 1 for all of the reactions investigated. Product ions arising from dissociative photoionization were attributed to the respective parent ion, as discussed in the results section. Each of the mass channels were corrected for the measured mass discrimination of the instrument.[28] Unfortunately, the majority of products reported here are not available commercially and are difficult to synthesize due to their high reactivity. As such, absolute photoionization cross-sections are not available from authentic standards, so photoionization cross-sections are estimated using the atom-pair additivity model of Bobeldijk et al.[29]

Reactant \ Product	-H•	-CH_3•
acetylene	1.0	
propyne	0.27	0.73
ethylene	1.0	
propene	0.14	0.86

Table 1 - Branching ratios derived from experimental measurements from the 1-iodopropynyl radical with the listed hydrocarbons. Values are corrected for mass discrimination and estimated photoionization cross-section. An absolute uncertainty of ±50% is estimated for these values.

The models of Bobeldijk et al. are empirically parameterized at 11.8 eV and 16.7 eV, higher than the photoionization energy used here (10.80 eV). The model can generate photoionization cross-sections with an uncertainty within the experimental error of ±20% at 16.7 eV, with a slightly larger uncertainty at 11.8 eV. Without photoionization spectra measured to 11.8 eV, extrapolation back to

10.80 eV is not possible. Nevertheless, we anticipate the relative cross-sections to be similar at 10.80 eV to those estimated at 11.80 eV. In general, the Bobeldijk models show that molecules of higher mass or more double or triple bonds to have a higher photoionization cross-section.[29] The absence of measured photoionization cross-sections means the following discussion and branching ratios shown in Table 1 rely on the assumptions described above. Taken together, we estimate an uncertainty in these cross-sections of ±50%.

For reaction of 1-propynyl with acetylene and ethylene, only a single product was measured that formed via H-loss from the respective initial adduct. Addition of 1-propynyl radical to d_4-propyne and propene resulted primarily in loss of methyl radical (73% and 86%, respectively), with the hydrogen loss channel contributing the remainder. Given that $^{\bullet}CH_3$ loss may only occur after addition of 1-propynyl radical to the internal acetylenic or vinylic carbon, this high $^{\bullet}CH_3$ yield suggests either that 1-propynyl radical has a propensity for addition to the internal carbon, or there is a significant flux through the three-membered ring intermediate that facilitates 1,2-propynyl transfer.

When competing β-scission or hydrogen elimination pathways follow after addition of 1-propynyl radical to propene or propyne, these reactions favor alkyl chain loss over hydrogen atom elimination. This result is supported by our quantum chemical calculations, which predict barriers for alkyl loss to be lower than that of hydrogen atom loss. Master equation modeling has the potential to further elucidate product branching, but this was outside the scope of the current work.

Kaiser and Mebel previously reported on the detailed hydrogen atom elimination dynamics of $^{\bullet}C_2H$ and $^{\bullet}CN$ radical reactions with acetylene, ethylene, propyne and propene via crossed-molecular beams experiments and master equation modeling.[30] In direct analogy to the reaction of 1-propynyl radical ($H_3CC{\equiv}C^{\bullet}$) reported in this contribution, experiment and theory suggest the reaction of $^{\bullet}C_2H$ and $^{\bullet}CN$ with acetylene and ethylene yield the addition-hydrogen elimination

products diacetylene or cyanoacetylene (c.f. penta-1,3-diyne) and vinyl acetylene or vinyl cyanide (c.f. pent-1-en-3-yne), respectively.[30,31]

Jamal and Mebel presented theoretical product branching ratios for the reaction of $^{\bullet}C_2H$ with propyne,[32] which revealed a significant $^{\bullet}CH_3$ elimination channel (21-61%) to form diacetylene that is consistent with the synchrotron-VUV photoionization mass spectrometry experiments of Goulay et al.[33] Reaction of the isoelectronic $^{\bullet}CN$ with propyne has been investigated by the crossed-molecular beams technique;[34] however, these experiments did not examine competition between hydrogen and methyl elimination channels. The theoretical investigation of Huang et al. predicted the major product formed from reaction of $^{\bullet}CN$ with propene was vinyl cyanide after $^{\bullet}CH_3$ elimination, consistent with the experimental measurements of Trevitt et al.[35,36] These results are similar to the Bouwman et al. investigation of $^{\bullet}C_2H$ + propene, where vinyl acetylene was the major product after $^{\bullet}CH_3$ elimination.

Implications for Titan

Current photochemical models of Titan's atmosphere assume hydrogen atom abstraction, hydrogen atom elimination, or simply "products", resulting from this class of reactions.[6,18] Table 2 presents branching via hydrogen loss reported previously for ethynyl radical and propynyl radical determined here with alkenes and alkynes.[31,33,37,38] These data demonstrate that molecular growth efficiency is decreased as alternative reaction channels to hydrogen elimination emerge. For example, when alkyl chains are located on double or triple bonds, alkyl radical loss dominates over hydrogen elimination.[31,33,37-39] The propensity of these reactions to generate alkyl radicals may further suggest a connection between the quantity of alkyl radicals and more reactive species such as ethynyl radical in vertical column profiles in Titan's atmosphere.

Neutral \ Radical	$^{\bullet}C_2H$	$H_3CC{\equiv}C^{\bullet}$
acetylene (C_2H_2)	1.0	1.0
propyne (C_3H_4)	0.3-0.5[33]	0.27
allene (C_3H_4)	0.7[33]	
1-butyne (C_4H_6)	0.3[38]	
ethylene (C_2H_4)	1.0[31]	1.0
propene (C_3H_8)	0.15[31]	0.14
1-butene (C_4H_{10})	0[37]	
2-butene (C_4H_{10})	0[37]	
isobutene (C_4H_{10})	0.39[37]	

Table 2 - Branching fractions of hydrogen loss channels during reaction of ethynyl radical ($^{\bullet}C_2H$) and 1-propynyl radical ($H_3CC{\equiv}C^{\bullet}$) with a range of alkenes and alkynes.

While the molecular growth efficiency observed here from reaction of 1-propynyl radical ($H_3CC{\equiv}C^{\bullet}$) and previously for ethynyl ($^{\bullet}C_2H$) and cyano radicals ($^{\bullet}CN$) with C_3-C_4 reactants is lower than assumed in current models, the reaction product formed in these reactions (e.g., penta-1,3-diyne in the case of 1-propynyl radical + propyne) contain terminal double and triple bonds that are susceptible to C-H homolysis. This mechanism is significant because the formation of terminal alkynes, for example, provides the potential for formation of larger ethynyl-like radicals where reaction rates near the collision limit are expected.

The primary motivation for this study is to further elucidate the complex chemistry driving formation of haze condensates in Titan's atmosphere. It is difficult to predict how incorporating the specific reactions investigated here into current photochemical models will impact the major reaction channels and product branching Titan's atmosphere. However, our work provides general evidence for the presence of additional reaction channels (beyond just H elimination commonly assumed in current Titan models) during the reaction of ethynyl-like radicals with trace hydrocarbons such as propene and propyne. In agreement with recent experiments identified above, this work challenges the assumption that simple radical addition/ hydrogen elimination reactions dominate during reactions with C_3 and larger unsaturated hydrocarbons. As such

we believe that our work challenges a number of assumptions commonly used in models of Titan's atmosphere.

Developing a master equation model based on these experiments to investigate the effect of temperature and pressure on the product branching ratios and the sensitivity of the reaction to the diluent gas and collisional energy transfer would be invaluable for aligning these results more closely with the environment in Titan's atmosphere. Work developing these models is in progress; however, it is beyond the scope of the current manuscript.

Conclusion

We have investigated the reaction of the ethynyl radical analogue, 1-propynyl radical, with a range of alkyne and alkene reagents at 300 K. The reaction of the 1-propynyl radical ($H_3CC{\equiv}C^{\bullet}$) with d_4-propyne (C_3D_4) and propene (C_3H_6) results primarily in methyl radical ($^{\bullet}CH_3$) elimination through prompt β-scission following addition to the double or triple bond. Our computational study is consistent with these results, which demonstrates that barriers to alkyl chain loss are typically lower than those of hydrogen atom elimination. These findings are similar to previous studies of both the cyano radical ($^{\bullet}CN$) + propene[35,40] reaction and ethynyl radical ($^{\bullet}C_2H$) + propene,[31] propyne,[33] butene[37] and butyne[38] reactions where alkyl radical loss was measured as a major reaction channel. Together, these results indicate that reactions of ethynyl-like radicals with large-chain unsaturated species result not only in larger, more unsaturated species, but can transfer a significant quantity of carbon to alkyl radicals. This result will influence the carbon cycling in Titan's atmosphere and implies that hydrogen atom production from ethynyl radical reaction with C_3 and larger molecules is overestimated in current models. These results demonstrate that a detailed analysis specifically targeting the identity of reaction products is crucial for accurately modeling molecular growth efficiency in Titan's atmosphere.

Acknowledgements

This work is supported by the National Aeronautics and Space Administration (NNH13AV43I). The Advanced Light Source is supported by the Director, Office of Science, Office of Basic Energy Sciences, of the U.S. Department of Energy under contract DE-AC02-05CH11231. JDS and DLO are supported by U.S. Department of Energy, Office of Science, Office of Basic Energy Sciences. Sandia is a multi-program laboratory operated by Sandia Corporation, a Lockheed Martin Company, for the National Nuclear Security Administration under contract DE-AC04-94AL85000. AJT is grateful to the Australian Research Council for funding through a Discovery Project (DP130100862). The authors thank Mr. Howard Johnson for technical support and Dr. Martin Fournier and Prof. Ian Sims for initial support during these experiments.

References

1 R. Lorenz and J. Mitton, *Titan unveiled: Saturn's mysterious moon explored*, Princeton University Press, New Jersey, 2008.
2 J. H. Waite, D. T. Young, T. E. Cravens, A. J. Coates, F. J. Crary, B. Magee and J. Westlake, *Science*, 2007, **316**, 870–875.
3 I. W. M. Smith, *Angew. Chem. Int. Ed. Engl.*, 2006, **45**, 2842–2861.
4 D. Carty, V. Le Page, I. R. Sims and I. Smith, *Chem. Phys. Lett.*, 2001, **344**, 310–316.
5 R. J. Hoobler and S. R. Leone, *J. Phys. Chem. A*, 1999, **103**, 1342–1346.
6 P. P. Lavvas, A. Coustenis and I. M. Vardavas, *Planetary and Space Science*, 2008, **56**, 27–66.
7 E. H. Wilson, *J. Geophys. Res.*, 2004, **109**, E06002.
8 V. Vuitton, R. V. Yelle and J. Cui, *J. Geophys. Res.*, 2008, **113**, E05007.
9 Y. Yang, Z. Li, Y. Zhao, S. Wan, H. Liu, X. Huang and C. Sun, *Comput. Theor. Chem.*, 2012, **991**, 66–73.
10 E. H. Wilson, *J. Geophys. Res.*, 2003, **108**, 5014.
11 A. J. Coates, F. J. Crary and G. R. Lewis, *Geophys Res Lett*, 2007, **34**, L22103.
12 M. López-Puertas, B. M. Dinelli, A. Adriani, B. Funke, M. García-Comas, M. L. Moriconi, E. D'Aversa, C. Boersma and L. J. Allamandola, *ApJ*, 2013, **770**, 132–8.
13 M.-C. Liang, Y. L. Yung and D. E. Shemansky, *ApJ*, 2007, **661**, L199–L202.
14 F. Raulin, *Space Sci Rev*, 2007, **135**, 37–48.
15 A. M. Mebel, V. V. Kislov and R. I. Kaiser, *J Am Chem Soc*, 2008, **130**, 13618–13629.
16 S. Harich, J. J. Lin, Y. T. Lee and X. Yang, *J. Chem. Phys.*, 2000, **112**, 6656–6665.
17 R. H. Qadiri, E. J. Feltham, N. Hendrik Nahler, R. Pérez Garc□a and M. N. R.

Ashfold, *J. Chem. Phys.*, 2003, **119**, 12842.
18 V. A. Krasnopolsky, *Icarus*, 2009, **201**, 226–256.
19 D. L. Osborn, P. Zou, H. Johnsen, C. C. Hayden, C. A. Taatjes, V. D. Knyazev, S. W. North, D. S. Peterka, M. Ahmed and S. R. Leone, *Rev. Sci. Instrum.*, 2008, **79**, 104103.
20 P. E. Crider, L. Castiglioni, K. E. Kautzman and D. M. Neumark, *J. Chem. Phys.*, 2009, **130**, 044310.
21 S. E. Wheeler, K. A. Robertson, W. D. Allen, H. F. Schaefer III, Y. J. Bomble and J. F. Stanton, *J. Phys. Chem. A*, 2007, **111**, 3819–3830.
22 D. L. Osborn, *Personal Communication, 2014*.
23 S. G. Lias, R. D. Levin and S. A. Kafafi, in *NIST Chemistry WebBook, NIST Standard Reference Database Number 69*, eds. P. J. Linstrom and W. G. Mallard, National Institute of Standards and Technology, Gaithersburg MD, 20899.
24 T. A. Cool, J. Wang, K. Nakajima, C. A. Taatjes and A. Mcllroy, *Int. J. Mass Spectrom.*, 2005, **247**, 18–27.
25 E. V. Shafir, I. R. Slagle and V. D. Knyazev, *J. Phys. Chem. A*, 2003, **107**, 8893–8903.
26 V. D. Knyazev and I. R. Slagle, *J. Phys. Chem. A*, 2002, **106**, 5613–5617.
27 S. G. Lias, in *NIST Chemistry WebBook, NIST Standard Reference Database Number 69*, eds. P. J. Linstrom and W. G. Mallard, Gaithersburg MD, 20899.
28 J. D. Savee, S. Soorkia, O. Welz, T. M. Selby, C. A. Taatjes and D. L. Osborn, *J. Chem. Phys.*, 2012, **136**, 134307.
29 M. Bobeldijk, W. J. Van der Zande and P. G. Kistemaker, *Chemical Physics*, 1994.
30 R. I. Kaiser and A. M. Mebel, *Chem. Soc. Rev.*, 2012, **41**, 5490–13.
31 J. Bouwman, F. Goulay, S. R. Leone and K. R. Wilson, *J. Phys. Chem. A*, 2012, **116**, 3907–3917.
32 A. Jamal and A. M. Mebel, *Phys. Chem. Chem. Phys.*, 2010, **12**, 2606–13.
33 F. Goulay, D. L. Osborn, C. A. Taatjes, P. Zou, G. Meloni and S. R. Leone, *Phys. Chem. Chem. Phys.*, 2007, **9**, 4291–4300.
34 L. C. L. Huang, N. Balucani, Y. T. Lee, R. I. Kaiser and Y. Osamura, *J. Chem. Phys.*, 1999, **111**, 2857–5.
35 A. J. Trevitt, S. Soorkia, J. D. Savee, T. S. Selby, D. L. Osborn, C. A. Taatjes and S. R. Leone, *J. Phys. Chem. A*, 2011, **115**, 13467–13473.
36 A. J. Trevitt, F. Goulay, G. Meloni and D. L. Osborn, *Int. J. Mass Spectrom.*, 2009.
37 J. Bouwman, M. Fournier, I. R. Sims, S. R. Leone and K. R. Wilson, *J. Phys. Chem. A*, 2013, **117**, 5093–5105.
38 S. Soorkia, A. J. Trevitt, T. M. Selby, D. L. Osborn, C. A. Taatjes, K. R. Wilson and S. R. Leone, *J. Phys. Chem. A*, 2010, **114**, 3340–3354.
39 A. Jamal, Florida International University, PhD Thesis, 2012.
40 K. L. Gannon, D. R. Glowacki, M. A. Blitz, K. J. Hughes, M. J. Pilling and P. W. Seakins, *J. Phys. Chem. A*, 2007, **111**, 6679–6692.